Neuron
NeuroResource

Single Action Potentials and Subthreshold Electrical Events Imaged in Neurons with a Fluorescent Protein Voltage Probe

Lei Jin,[1,7] Zhou Han,[1,2,7] Jelena Platisa,[2,3] Julian R.A. Wooltorton,[4] Lawrence B. Cohen,[1,5,*] and Vincent A. Pieribone[1,2,6,*]
[1]Cellular and Molecular Physiology, Yale University School of Medicine, New Haven, CT 06511, USA
[2]The John B. Pierce Laboratory, Inc., New Haven, CT 06519, USA
[3]Faculty of Physical Chemistry, University of Belgrade, Republic of Serbia
[4]Department of Neuroscience, Perelman School of Medicine at the University of Pennsylvania, Philadelphia, PA 19104, USA
[5]Center for Functional Connectomics, Korea Institute of Science and Technology, Seoul 136-791, Republic of Korea
[6]Neurobiology, Yale University School of Medicine, New Haven, CT 06511, USA
[7]These authors contributed equally to this work
*Correspondence: lawrence.cohen@kist.re.kr (L.B.C.), vpieribo@jbpierce.org (V.A.P.)
http://dx.doi.org/10.1016/j.neuron.2012.06.040

SUMMARY

Monitoring neuronal electrical activity using fluorescent protein-based voltage sensors has been limited by small response magnitudes and slow kinetics of existing probes. Here we report the development of a fluorescent protein voltage sensor, named ArcLight, and derivative probes that exhibit large changes in fluorescence intensity in response to voltage changes. ArcLight consists of the voltage-sensing domain of Ciona intestinalis voltage-sensitive phosphatase and super ecliptic pHluorin that carries the point mutation A227D. The fluorescence intensity of ArcLight A242 decreases by 35% in response to a 100mV depolarization when measured in HEK293 cells, which is more than five times larger than the signals from previously reported fluorescent protein voltage sensors. We show that the combination of signal size and response speed of these new probes allows the reliable detection of single action potentials and excitatory potentials in individual neurons and dendrites.

INTRODUCTION

A genetically encoded sensor of membrane potential was first introduced by Siegel and Isacoff (1997) as a fusion between the Shaker potassium channel and wild-type green fluorescent protein from Aequorea victoria (aqGFP). Subsequent ion channel-based voltage sensors were designed to include a single fluorescent protein (FP; Ataka and Pieribone, 2002) or FPs that form Förster resonance energy transfer pairs (FRET; Sakai et al., 2001b). However, these early probes failed to show significant membrane localization in mammalian cells (Baker et al., 2007, 2008). Later sensors based on the voltage-sensing domain of Ciona intestinalis voltage-sensitive phosphatase (CiVSP; Murata et al., 2005) produced robust signals in mammalian cells (Dimitrov et al., 2007; Tsutsui et al., 2008). We and others have combined many Ciona intestinalis voltage sensor (CiVS) with different FPs to produce FP voltage sensors with improved properties (Dimitrov et al., 2007; Baker et al., 2008; Tsutsui et al., 2008; Perron et al., 2009; Jin et al., 2011). However, to date this approach had not yielded probes with the necessary combination of signal size and speed that would make it possible to image individual voltage signals (i.e., action potentials or subthreshold potentials) in neurons.

Here we report the development of an FP voltage sensor, named ArcLight, which is based on a fusion of the CiVS and the fluorescent protein super ecliptic pHluorin that carries an A227D mutation. The phosphatase domain of the CiVSP is deleted in all our probes. We show that ArcLight A242, a probe derived from ArcLight, responds to a 100mV depolarization with signals more than five times larger than previously reported CiVS-based FP voltage sensors, including Mermaid (Tsutsui et al., 2008) and the VSFPs (Lundby et al., 2008; Akemann et al., 2010). We also show that ArcLight and its derivative probes can detect individual action potentials and subthreshold electrical events in cultured mammalian neurons in single trials with widefield fluorescent light microscopy.

RESULTS AND DISCUSSION

To study the effect of using different FPs in CiVS-based FP voltage sensors, we replaced the FRET pair (mUKG and mKOk) in the Mermaid probe (Tsutsui et al., 2008) with ecliptic pHluorin (GenBank: AAC40226.1; Miesenböck et al., 1998). Ecliptic pHluorin was engineered by introducing six mutations to the wild-type aqGFP (Miesenböck et al., 1998). The pH/fluorescence intensity profile of ecliptic pHluorin is basic-shifted with respect to the parent aqGFP (Miesenböck et al., 1998). While the FP voltage sensor containing ecliptic pHluorin exhibited a small voltage-dependent change in fluorescence intensity (−1.3% ± 0.3% ΔF/F) to a +100mV voltage step (Figures 1A and 1B), we discovered in one stable HEK293 cell line an unintended point mutation, A227D (following the numbering of wild-type aqGFP residues; Figure S1A available

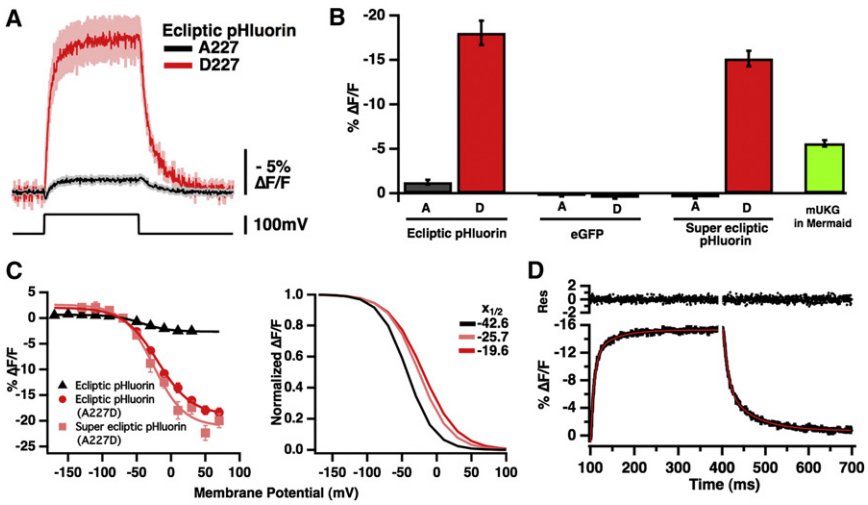

Figure 1. The A227D Mutation Increases the Fluorescence Response Magnitude of CiVS-Based Voltage Sensors Containing Ecliptic pHluorin or Super Ecliptic pHluorin

(A) Changes in fluorescence intensity in HEK293 cells expressing either CiVS-ecliptic pHluorin (black, n = 9 cells; 10 trials for each cell) or CiVS-ecliptic pHluorin A227D (red, n = 6) in response to 100mV depolarizing pulses (−70mV holding potential). The lighter traces (gray and pink) indicate the standard error of the data.

(B) The fractional fluorescence change % ΔF/F (mean ± SEM) produced by 100mV depolarization steps in seven FP voltage sensors with different FPs inserted at S249 of the CiVS: ecliptic pHluorin (black; n = 9), ecliptic pHluorin A227D (red; n = 6), eGFP (black; n = 10), eGFP A227D (black; n = 5), super ecliptic pHluorin (black; n = 9), super ecliptic pHluorin A227D (ArcLight, red; n = 8), and the mUKG emission of Mermaid (green; n = 25).

(C) Left: peak % ΔF/F (mean ± SEM) versus membrane potential and fitted Boltzmann curves for three CiVS-based FP voltage sensors containing different FPs: ecliptic pHluorin (black), ecliptic pHluorin A227D (red), and super ecliptic pHluorin A227D (ArcLight, pink). Right: Boltzmann-fits of normalized fluorescence change of the three probes.

(D) Bottom: the fluorescence change of super ecliptic pHluorin A227D (ArcLight) during depolarization (left) and repolarization (right) using a 100mV depolarization step from −70mV (black, single trial) and a double exponential curve fit (red). Top: residual versus time for the on and off fitted curves.

online), within the inserted ecliptic pHluorin. The mutant sensor produced a 14-fold increase (−18.1% ± 0.3%, n = 6) in ΔF/F (Figures 1A and 1B) per 100mV. This fractional fluorescence change is ~3 times larger than current CiVS-based FP voltage sensors (Lundby et al., 2008; Tsutsui et al., 2008; Akemann et al., 2010).

We sought to determine whether the large response magnitude imparted by the A227D mutation could be reproduced in other FP voltage sensors. We examined the effects of the A227D mutation on FP voltage sensors containing either super ecliptic pHluorin (Sankaranarayanan et al., 2000) or eGFP. These two FPs are closely related and were both derived from the wild-type aqGFP. Super ecliptic pHluorin contains two eGFP-like mutations, F64L and S65T, in addition to mutations found in ecliptic pHluorin (Sankaranarayanan et al., 2000; Figure S1A). The two eGFP-like mutations simplify the excitation spectra of super ecliptic pHluorin to a single peak (~490 nm) and produce a brighter and more photo-stable FP that retains the basic-shifted pH/fluorescence intensity profile (Sankaranarayanan et al., 2000). The FP voltage sensors containing either super ecliptic pHluorin or eGFP do not produce substantial ΔF with depolarizing steps (Figure 1B). However, introducing the A227D mutation dramatically increased the response magnitude of the super ecliptic pHluorin containing sensor (Figure 1B). In contrast, introducing the A227D mutation did not increase the response magnitude of the sensor containing eGFP (Figure 1B). Cells expressing probes containing super ecliptic pHluorin A227D were brighter than ones expressing ecliptic pHluorin A227D (3460 ± 609 AU, n = 12 cells versus 373 ± 40 AU, n = 11 cells, respectively); however, the bleach rates were not significantly different (−4.8% ± 0.8% versus −6.4% ± 0.7% over 2 s of laser illumination). We conclude from these results that the mutations found in ecliptic pHluorin are required for the A227D mutation to confer its effect. However, the dual peak excitation spectrum of ecliptic pHluorin is not required for the enhanced response.

The FP voltage sensor containing the super ecliptic pHluorin A227D was named ArcLight. The A227D mutation did not alter the level of expression of the probes at the plasma membrane or the basal cellular fluorescence level in HEK293 cells (data not shown). We purified free recombinant protein of super ecliptic pHluorin and super ecliptic pHluorin A227D from bacteria and compared the photophysical properties of these two proteins. We found that the A227D mutation did not alter the excitation or emission spectrum or pH sensitivity of super ecliptic pHluorin (Figure S2). The A227D mutant retained a sigmoidal fluorescence-voltage relationship with a large increase in amplitude and a small leftward shift in $V_{1/2}$ (Figure 1C). The kinetics of the fluorescence responses were also similar. We determined that the "on" kinetics of ArcLight in response to a +100mV step were best fit by a double exponential curve (Figure 1D and Figure S3A), with the time constant (tau, τ) of the fast component of ~10 ms and τ of the slow component of ~50 ms (Figure S3B).

Super ecliptic pHluorin differs from eGFP at nine positions: 80, 147, 149, 163, 175, 202, 204, 206, and 231, out of 238 residues (Figure S1). All but one (163) of the nine residues have outward-facing side chains on the surface of the FP and many of the nine residues reside on the same side of the beta barrel (Figure 2A) as A227. We wanted to determine which of these nine amino acids are important for the A227D mutation to exert the increase signal in ArcLight. We introduced single point mutations in six variant constructs of ArcLight, replacing the most dissimilar residues in super ecliptic pHluorin with those in eGFP: R80Q, D147S, Q149N, F202S, T204Q, and T206A (Figure 2A). While the R80Q or Q149N mutations did not alter the response magnitude of ArcLight, the D147S mutation caused a large decrease in the signal size, and the F202S and T204Q mutations nearly eliminated the

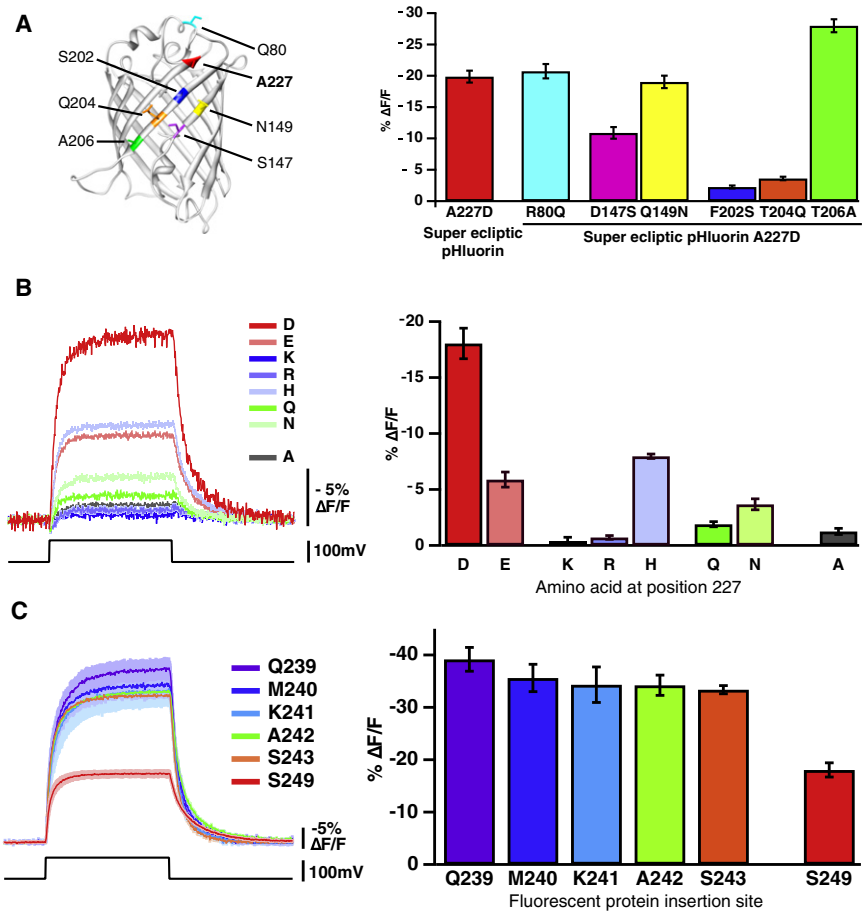

Figure 2. The Modulatory Effect of the A227D Mutation Is Dependent on a Negative Charge at that Position and on Other Surface Residues of the FP

A larger response magnitude was achieved when the FP was relocated closer to the S4 domain of the CiVS. All responses are produced by +100mV voltage steps in HEK293 cells.

(A) Left: the 3D structure of eGFP (PDB identifier 1EMG) illustrating the position of residues in super ecliptic pHluorin (ArcLight) that were mutated to those found in eGFP: Q80 (cyan), S147 (magenta), N149 (yellow), S202 (blue), Q204 (orange), and A206 (green). The A227D mutation is marked with red. Right: the fractional fluorescence change, % ΔF/F (mean ± SEM), of seven CiVS-based voltage sensors containing different mutations of super ecliptic pHluorin inserted at S249 of the linker. These modifications were mutations of super ecliptic pHluorin (A227D) at the sites indicated in the left panel. ArcLight (red, n = 10), ArcLight with single point mutations: R80Q (cyan, n = 6), D147S (magenta, n = 7), Q149N (yellow, n = 6), F202S (blue, n = 8), T204Q (orange, n = 8) and T206A (green, n = 6). A single trial was recorded from each cell and the peak values of these trials were averaged.

(B) Left: averaged optical traces of CiVS-ecliptic pHluorin and seven mutant probes carrying different point mutations at residue 227 of the FP. CiVS-ecliptic pHluorin (A, gray, n = 9). Point mutations at residue 227: A227D (red, n = 6), A227E (pink, n = 8), A227K (dark blue, n = 4), A227R (intermediate blue, n = 8), A227H (light blue, n = 6), A227Q (green, n = 5), or A227N (light green, n = 9). Ten trials were averaged for each cell and then the values from the different cells averaged. Right: summary of the peak % ΔF/F (mean ± SEM) for probes in the left panel.

(C) Left: averaged optical traces of ArcLight and ArcLight-derived probes with super ecliptic pHluorin A227D moved to different locations within CiVS: ArcLight Q239 (purple, n = 7), ArcLight M240 (blue, n = 8), ArcLight K241 (cyan, n = 7), ArcLight A242 (green, n = 7), ArcLight S243 (orange, n = 7), and ArcLight (S249; red, n = 10). A single trial was recorded from each cell and the optical traces of these trials were averaged. Right: summary of the peak % ΔF/F (mean ± SEM) for probes in the left panel.

ArcLight response (Figure 2A). Conversely, the T206A mutation increased the signal size.

We also explored whether replacing the A227 in ecliptic pHluorin with amino acids other than aspartic acid would modulate the response of the probe. We found that replacement of A227 with glutamic acid enhanced the ΔF/F response over A227; however, this was a significantly smaller increase than that seen with aspartic acid (Figure 2B). Basic residues (i.e., arginine and lysine) at position 227 eliminated the voltage-dependent fluorescence change (Figure 2B). These findings indicate that the presence of a negative charge at position 227 is essential for the increase in fluorescence response magnitude but the single additional carbon present in the glutamic acid side chain reduces this effect. Replacement of A227 with polar residues (i.e., histidine, glutamine, or asparagine) also improved the fluorescence response, but not as much as aspartic acid (Figure 2B).

Moving an FP to different positions along the linker between the CiVS and the phosphatase has been shown to alter the signal size and response speed of the resulting probes (Baker et al., 2008). We sought to determine whether the improvement in response magnitude caused by the A227D mutation persists when the FP is placed after sites other than S249 of the linker. Five new probes were engineered with super ecliptic pHluorin A227D relocated closer to the S4 domain of the CiVS, after amino acids Q239, M240, K241, A242, or S243 (Figure S1B). Each of the five derivatives of ArcLight resulted in a further increase of the response magnitude (~35% versus ~18% ΔF/F) to a 100mV depolarization step (Figure 2C). Thus the large improvement of signal size seen with this mutation is not limited to a specific location along the linker segment; an even greater increases in signal size was achieved by moving the FP closer to the S4 domain.

Optical methods offer the promise of less invasive, better targeted, and greater multisite monitoring of neuronal activities compared to traditional electrode-based methods. A number of FP-based, self-contained probes of membrane potential have been described (Siegel and Isacoff, 1997; Sakai et al., 2001a; Ataka and Pieribone, 2002; Baker et al., 2007; Dimitrov et al., 2007; Lundby et al., 2008; Tsutsui et al., 2008). While

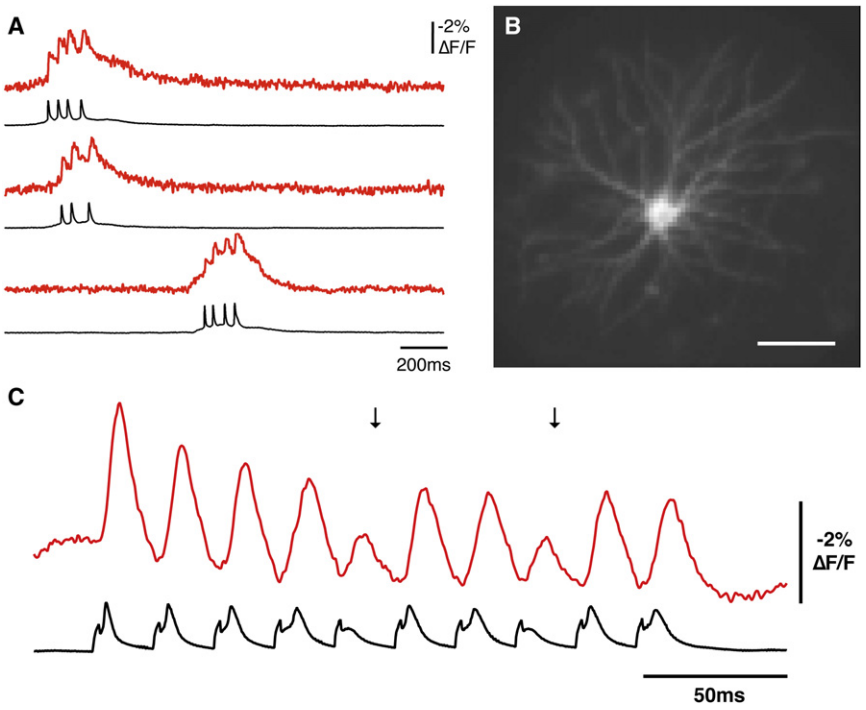

Figure 3. Detection of Action Potentials in Neurons with the ArcLight A242 Probe

(A) Sample traces of single trial recordings of spontaneous action potential bursts from the neuron shown in (B). All optical traces have double exponential subtraction of bleach and were low pass filtered with a Kaiser-Bessel 30 filter (200 Hz cut off).

(B) An 80 × 80 depixelated image of the neuron presented in (A). Scale bar: 50 μm.

(C) The optical and voltage recording of a stimulated action potential burst from a different neuron expressing the ArcLight A242 probe. All traces have double exponential subtraction of bleach and used a Binomial smoothing of one and a τ of four.

FP-based voltage sensors may perform well in cell lines (i.e., HEK293, PC12, etc.), it has been challenging in many cases to transfer probes into neurons and still observe detectable responses (Akemann et al., 2010). All of the FP-based probes cited above suffered from one or more problems, including low intensity of probe fluorescence in neurons, small response magnitudes, slow kinetics of the fluorescence response, and poor membrane versus intracellular localization (Perron et al., 2009). To date none of these have convincingly demonstrated detection of individual action potentials and postsynaptic potentials in neurons. When expressed in neurons, the signal-to-noise ratio for action potential detection using these probes has been poor (Baker et al., 2007; Perron et al., 2009).

Expression of ArcLight and its derivatives in cultured mouse hippocampal neurons produced brightly fluorescent cells (Figures 3–5; Figure S4A) with expression both in the soma and dendrites (Figure S4A). In dendrites it appears largely membrane localized (Figure S4A). The probe did not appear to dramatically alter neuronal excitability as electrical recordings of spontaneous action potentials in nontransfected, mock-transfected, and ArcLight-transfected neurons had widths and amplitudes that were not significantly different (Figures S4B and S4C). The probe also did not appear to cause excessive phototoxicity as spontaneous action potentials of similar properties could be observed following at least 4 min (longest period tested) of excitation (Figure S4D). In spite of the relatively slow response of the probe in HEK293 cells (fast $\tau \sim 10$ ms), we could optically detect spontaneous (Figure 3A) and evoked action potentials (Figure 3C) in neurons expressing the ArcLight probes. The response appeared as a −1 to −5% ΔF/F (−3.2% ± 2.2%, n = 20 cells) change in the fluorescence intensity. As expected, this ΔF/F is smaller than those from longer duration voltage steps in HEK293 cells (Figures 1 and 2). Similarly, action-potential-shaped voltage steps in HEK293 cells also resulted in smaller amplitude signals (Figure S5). The fluorescence change did not return to baseline between action potentials during high-frequency trains (Figure 3A), because of the slow component of the probe's response to voltage changes. However, individual action potentials were still clearly detectable (Figure 3). Much smaller-amplitude, subthreshold electrical events (probably excitatory postsynaptic potentials) were readily detectable with several ArcLight probes, including ArcLight Q239 and A242 (Figures 4 and 5A). The longer duration of these events compared to action potentials enhances their detectability. In addition, individual depolarizations arising from action potentials and subthreshold events were evident in distal dendritic segments, recorded with ArcLight Q239 (Figure 5). Expression of ArcLight or its derivatives did not appear to affect the amplitude and duration of action potentials produced in neurons when compared to mock-transfected neurons (Figure S4D). We are presently attempting to use lentivirus and adeno-associated virus (AAV) to express ArcLight constructs in vivo.

It is not clear how the A227D mutation caused the dramatic increase in the fluorescence response magnitude of ArcLight to voltage changes. D227 may interact with the membrane, other residues in the FP, or the linker connecting the FP to the S4 domains of CiVS. It is also possible that D227 remains un-ionized and is associated with the inner plasma membrane. The shifted pH sensitivity of the background ecliptic pHluorin or super ecliptic pHluorin proteins may be necessary to enable the modulatory effect of D227. While we showed that the A227D mutation does not alter the excitation or emission spectrum or pH sensitivity of the free FP, it does alter the local charge on one side of the FP surface that may be important for imparting voltage modulation. D227 may act as a "local acid" and reversibly protonate residues T203 and/or H148, which have been shown to be affected by pH (Brejc et al., 1997; Elsliger et al., 1999) or it may alter proton movements across the surface and within the beta barrel of the FP (Agmon, 2005; Shinobu et al., 2010). The fact that aspartic acid, an acidic amino acid which is

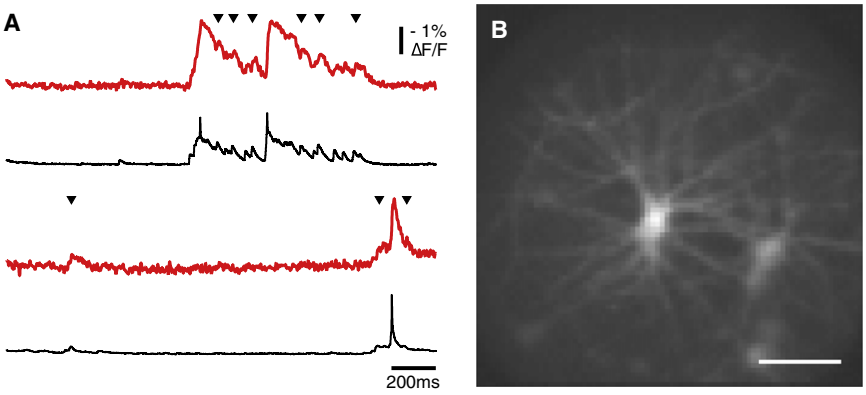

Figure 4. Detection of Subthreshold Depolarizations in Neurons with the ArcLight Q239 Probe

(A) Sample traces of single trial recordings of spontaneous subthreshold and action potential activity from the neuron shown in (B). All optical traces have double exponential subtraction of the bleach and are low pass filtered with a Kaiser-Bessel 30 filter (200 Hz cut off). The arrowheads indicate the depolarizations (likely EPSPs) that triggered visible changes in the optical recordings. (B) An 80 × 80 depixelated image of the neuron presented in (A). Scale bar: 50 μm.

sterically small in size, caused greater modulatory effect than any other amino acid tested at the crucial 227 site supports the "local acid" hypothesis. In addition, the modulatory effect of the A227D mutation appears to depend on several other residues that are present only in ecliptic pHluorin as introducing the A227D mutation alone in eGFP did not increase the response magnitude of that probe. The spatial proximity of these necessary residues on one surface of the beta barrel (Figure 2A) suggests that this surface interacts with an external factor that is necessary for fluorescence modulation.

The slow temporal response of ArcLight suggests that the change in fluorescence intensity is linked to a secondary rearrangement in the voltage sensor following the voltage change but not directly to the rapid gating charge movements (Villalba-Galea et al., 2009). Moreover, the sigmoidal shape of the voltage/fluorescence response curve of ArcLight indicates that the process is associated with rearrangements arising from gating charge movements and that the chromophore is not directly affected by changes in the voltage field (like a traditional small molecule organic voltage-sensitive dye). The nonlinearity and slow kinetics of ArcLight do not allow detailed studies of action potential shape and propagation within a single cells as is possible with small molecule organic voltage dyes (e.g., Popovic et al., 2011) but do allow action potential detection with lower bandwidth recording.

Voltage sensors based on GFP-like fluorescent proteins offer the advantage of substantially greater brightness when compared to other spontaneously fluorescent proteins (Kralj et al., 2011, 2012). While sensors based on microbial rhodopsins have shown promise in terms of far red-shifted spectrum and relative response magnitude, the brightness of these probes is dramatically lower than GFP-based probes. Arch D95N has a quantum yield of 0.0004 (Kralj et al., 2012) versus 0.54 for eGFP (Ilagan et al., 2010). In addition the on rate of the nonconducting rhodopsin-based probe (i.e., Arch D95N) is four times slower than ArcLight probes (41 ms for Arch D94N (Kralj et al., 2012) versus ~10 ms for the fast component of ArcLight).

The large modulatory effect imparted by the D227 mutation introduces the concept of tuning the FP in FP-based voltage sensors as a way to improve them. Previous studies have made changes to the types of FPs or locations of FPs but have not attempted to modify the FP as a way to improve a probe's characteristics. In the present study, a small collection of mutations in the FP dramatically increases the change of its fluorescence intensity in response to voltage-induced movements in CiVS. However, these mutations do not alter obvious biophysical properties (i.e., the excitation and emission spectra, pH sensitivity) that would have allowed identification a priori using traditional mutagenesis and screening in *E. coli*. Mutated sensors still need to be screened in eukaryotic cells in which constructs traffic to the plasma membrane and the resting membrane potential can be set and altered.

The ArcLight sensors do not utilize FRET between two fluorescent proteins to produce a signal and it functions at several different insertion sites within the CiVS. ArcLight and its derivatives represent a very substantial improvement in the signal size of a FP voltage sensor, providing a protein-based method to monitor action potentials and subthreshold depolarization in neurons and potentially other cells and organelles.

EXPERIMENTAL PROCEDURES

Molecular Biology

Initially, DNA constructs were generated by replacing the FRET pairs (mUKG and mKOk) in a CiVS (R217Q) -based probe, i.e., Mermaid (Tsutsui et al., 2008), with ecliptic pHluorin (Miesenböck et al., 1998). The coding sequence of the pHluorin was amplified with the polymerase chain reaction (PCR) using the pfu DNA polymerase (Agilent Technologies, CA), digested with restriction enzymes BamHI and XbaI and inserted into the corresponding sites of the Mermaid construct. Primers used in PCR reaction were 5′-CGCGGATCCCATGAGTAAAGGAGAAGAACTTTTCACTGGAG-3′ and 5′-GCGTCTAGATCATTTGTATAGTTCATCCATGCCATGTGTAATCC-3′. Point mutations and modification to the linker sequences between the CiVS (R217Q) and ecliptic pHluorin were introduced by using the QuickChange II XL site-directed mutagenesis kit (Agilent Technologies, CA). All DNA constructs were verified by sequencing using the dye-termination method (W. M. Keck Foundation, Biotechnology Resource Laboratory, Yale University, CT).

Fluorescent Protein Purification

Expression constructs were generated by inserting PCR-amplified fragments of super ecliptic pHluorin or super ecliptic pHluorin A227D cDNA into the pCR4Blunt TOPO vector (Invitrogen, NY). This procedure introduces a 6xHis tag to the N terminus of the fusion proteins to allow affinity purification. Top10 bacteria (Invitrogen, NY) were transformed with the expression constructs and fusion proteins were purified with His-Select Nickel Affinity Gel (Sigma-Aldrich, MO), following the manufacturer's instructions. The purified proteins were concentrated with Amicon Ultra-15 centrifugal filters

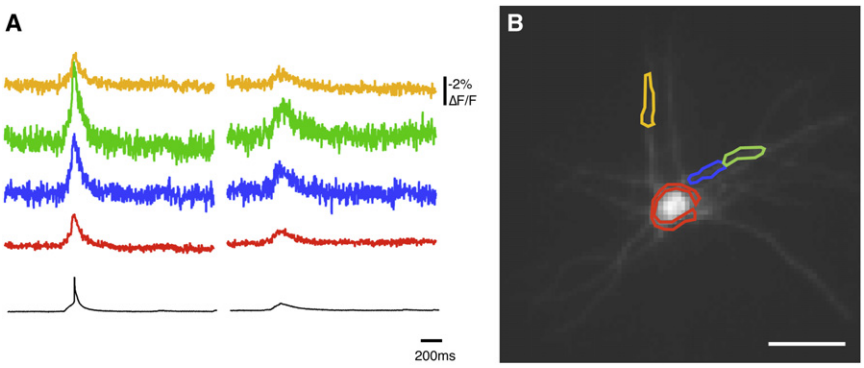

Figure 5. Detection of Subthreshold Events and Action Potentials in the Soma and Dendrites of a Neuron with the ArcLight Q239 Probe

(A) Sample traces of single trial recordings of action potential (left panel) and subthreshold events (right panel) from four locations of the neuron in (B). Optical recordings (colored): % ΔF/F from the area of interest in the same color in (B); soma electrode voltage recordings (black). All optical traces have double exponential subtraction of the bleach and are low pass filtered with a Kaiser-Bessel 30 filter (200 Hz cut off).

(B) An 80 × 80 image of a neuron presented in (A) with the regions of interest averaged to produce the traces shown in (A). Scale bar: 50 μm.

(MWCO 10,000, Millipore, MA), dialyzed against 100 mM sodium phosphate buffer, pH 7.4, and stored at 4°C.

Spectrofluorimetry

Absorption spectra of the purified fusion proteins were measured with a Shimadzu UV-1601PC UV-VIS spectrophotometer (Shimadzu, Japan). Fluorescence excitation and emission spectra of the fusion proteins were measured with a Horiba Jobin Yvon Fluorolog 3 spectrophotometer). In order to determine pH-dependent fluorescence, purified proteins were diluted to a concentration of 0.36 μM in pH-adjusted buffers containing 100 mM NaCl, 1 mM $CaCl_2$, and 1 mM $MgCl_2$. The pH of the buffers was adjusted with MES (for pH 3.5, 4.5, and 5.5), HEPES (for pH 6.5 and 7.5), or Bicine (for pH 8.5 and 9.5) to a final concentration of 25 mM of these chemicals. To determine the protein concentration, the protein was denatured in 0.1N NaOH and absorption was measured at 280 nm was measured using a Beckman Coulter DU 730 uv/vis spectrophotometer (Beckman Coulter, CA). The protein concentration was calculated using a 20,010 M^{-1} cm^{-1} extinction coefficient for both super ecliptic pHluorin and super ecliptic pHluorin A227D.

Cell Culture

HEK293 cells (AATC, VA) were maintained in Dulbecco's Modified Eagle Medium (High Glucose; DMEM; Invitrogen, NY) supplemented with 8% fetal bovine serum (FBS; Sigma-Aldrich, MO). Hippocampal neurons were isolated from E18 mouse embryos and maintained in Neurobasal medium with 0.5 mM Glutamax-I and 1 ml of B-27 supplement (Invitrogen, NY) per 50 ml of cultured medium. Cells were plated on coverslips coated with poly-L-lysine (Sigma-Aldrich, MO) and kept in an incubator at 37°C with 5% CO_2. Transient transfection was accomplished by using half of the manufacturer's recommended amount of DNA (2 μg per 35 mm dish or 0.4 μg per 12 mm coverslip in 24-well dish) and Lipofectamine 2000 (5 μl per 35 mm dish or 1 μl per 12 mm coverslip; Invitrogen, NY).

Electrophysiology

Microelectrode recordings were performed in a perfused chamber with the bath temperature kept at 33°C–35°C by a temperature controller. The bath solution contained 150 mM NaCl, 4 mM KCl, 2 mM $CaCl_2$, 1 mM $MgCl_2$, 5 mM D-glucose, and 5 mM HEPES, pH 7.4. We used 3–5 MΩ glass patch pipettes (capillary tubing with 1.5/0.75 mm OD/ID-World Precision Instruments, FL) that were pulled on a P-97 Flaming/Brown type micropipette puller (Sutter Instrument Company, CA). The pipette solution contained 120 mM K-aspartate, 4 mM NaCl, 4 mM $MgCl_2$, 1 mM $CaCl_2$, 10 mM EGTA, 3 mM Na_2ATP, and 5 mM HEPES, pH 7.2. Voltage-clamp recordings in the whole-cell configuration were performed using a Patch Clamp PC-505B amplifier (Warner Instruments, CT) with a holding potential of −70mV. Spontaneous activity of cultured hippocampal neurons was recorded in current clamp mode without holding current injection. For stimulation experiments, action potentials were evoked by a 2 ms current injection. The pipette solution for neuron recordings contained 120 mM K-gluconate, 3 mM KCl, 7 mM NaCl, 4 mM Mg-ATP, 0.3 mM Na-GTP, 20 mM HEPES, and 14 mM Tris-phosphocreatin (pH adjusted with KOH to pH 7.3) (Popovic et al., 2011).

Wide-Field Imaging

Whole-cell patch-clamped cells were imaged either with a Nikon Eclipse E6000FN upright microscope with a water immersion objective, Nikon Fluor 60×/1.00 N.A., or with a Nikon Eclipse TE300 inverted microscope with a 60×/1.40 N.A. oil immersion objective lens (Nikon, NY). For data collected with a 150 W Xenon arc lamp (Opti Quip, NY), we used two filter sets either an excitation filter HQ480/30X, a dichroic mirror 505DCXR and an emission filter HQ510LP (Chroma, Bellows Falls, VT) or GFP-3035B filter cube with an excitation filter 472/30 nm, dichroic mirror 495 nm, and emission filter 520/35 nm (Semrock, Rochester, NY). For data recorded with laser illumination, either a MLL-III-473 nm 50 mW or a MLL-FN-473 nm 50 mW (Changchun New Industries Optoelectronics Tech. Co., China) was used. The laser light was transmitted into the microscope by a multimode fiber coupler (Siskiyou, OR), a quartz light guide, and an Achromatic EPI-Fluorescence Condenser (Till Photonics, NY). For laser illumination, the excitation filter was removed from the filter cube. The fluorescence image was demagnified by an Optem zoom system, A45699 (Qioptiq LINOS Inc, NY), and projected onto the 80 × 80 pixel chip of a NeuroCCD-SM camera controlled by NeuroPlex software (RedShirtImaging, GA). The images were recorded at a frame rate of 1000 fps for HEK293 cells and at 2000 fps for neuron measurements. When we used laser excitation the recordings were from single trials.

Confocal Imaging

Confocal images were obtained with a Zeiss 780 LSM (Carl Zeiss AG, Germany) confocal laser scanning microscope using a Plan-Apochromat 63x/1.40 Oil DIC M27 objective. A 488 nm wavelength Argon laser was used for excitation. The dichroic beam splitter was a MBS 488. The emission filter was 493–598 nm. Zeiss Zen 2009 software was used for image acquisition and processing.

Data Processing

NeuroPlex software (RedShirtImaging, GA) was used to view the image sequences and output optical and electrophysiological recordings. The % ΔF/F was calculated by first subtracting the dark image from all frames; then the average of a region of interest in each frame (F) is subtracted from the average of the region taken from ten frames prior to the event of interest (F_0) and this value is then divided by F_0, i.e., % ΔF/F = ((F − F_0) / F_0) × 100. The data were further processed and statistically analyzed with Origin8.1 (OriginLab, MA), LabView (National Instruments, TX), Igor Pro 6 (Wavemetrics, OR), and Excel (Microsoft, WA).

The probe dynamics are fitted with either a single exponential equation,

$$y = y_0 + a_1 e^{-(x-x_0)/\tau_1},$$

or a double exponential equation,

$$y = y_0 + a_1 e^{-(x-x_0)/\tau_1} + a_2 e^{-(x-x_0)/\tau_2}.$$

The ΔF/F versus V plot was analyzed with the Boltzmann equation:

$$y = a_2 + \frac{a_2 - a_1}{1 + e^{(x - x_{1/2})/s}}.$$

The normalized ΔF/F versus V plot is calculated from the Boltzmann fit:

$$y = \frac{1}{1 + e^{(x - x_{1/2})/s}}$$

where a_1 and a_2 are constants, τ_1 and τ_2 are time constants in ms, $x_{1/2}$ is the membrane potential in mV at half maximal ΔF/F, and s is the slope.

SUPPLEMENTAL INFORMATION

Supplemental Information includes five figures and can be found with this article online at http://dx.doi.org/10.1016/j.neuron.2012.06.040.

ACKNOWLEDGMENTS

This work was supported by the National Institutes of Health (U24NS057631, DC005259-39, ARRA U24NS057631-03S1, and ARRA-R01NS065110), the World Class Institute program of the National Research Foundation of Korea, Grant Number: WCI 2009-003), and The John B. Pierce Laboratory. The authors thank Dr. Leslie M. Loew and Dr. Ping Yang at the University of Connecticut Health Center for assistance in the determination of the physiochemical characteristics of fluorescent proteins. We would like to thank Marko Popovic for technical assistance with imaging. These studies were performed as part of an NIH Cooperative Agreement (U24) Work Group that consisted of the authors and the laboratories of Thomas Hughes, Brian Salzberg, and Ehud Isacoff. We would also like to thank our NIH Program Officer Randall Stewart. We would also like to thank the technical staff of the John B. Pierce Laboratory, John Buckley, Richard Rascati, Ron Goodman, Andrew Wilkens, Angelo DiRubba, and Tom D'Alessandro.

Accepted: June 22, 2012
Published: September 5, 2012

REFERENCES

Agmon, N. (2005). Proton pathways in green fluorescence protein. Biophys. J. *88*, 2452–2461.

Akemann, W., Mutoh, H., Perron, A., Rossier, J., and Knöpfel, T. (2010). Imaging brain electric signals with genetically targeted voltage-sensitive fluorescent proteins. Nat. Methods *7*, 643–649.

Ataka, K., and Pieribone, V.A. (2002). A genetically targetable fluorescent probe of channel gating with rapid kinetics. Biophys. J. *82*, 509–516.

Baker, B.J., Lee, H., Pieribone, V.A., Cohen, L.B., Isacoff, E.Y., Knopfel, T., and Kosmidis, E.K. (2007). Three fluorescent protein voltage sensors exhibit low plasma membrane expression in mammalian cells. J. Neurosci. Methods *161*, 32–38.

Baker, B.J., Mutoh, H., Dimitrov, D., Akemann, W., Perron, A., Iwamoto, Y., Jin, L., Cohen, L.B., Isacoff, E.Y., Pieribone, V.A., et al. (2008). Genetically encoded fluorescent sensors of membrane potential. Brain Cell Biol. *36*, 53–67.

Brejc, K., Sixma, T.K., Kitts, P.A., Kain, S.R., Tsien, R.Y., Ormö, M., and Remington, S.J. (1997). Structural basis for dual excitation and photoisomerization of the Aequorea victoria green fluorescent protein. Proc. Natl. Acad. Sci. USA *94*, 2306–2311.

Dimitrov, D., He, Y., Mutoh, H., Baker, B.J., Cohen, L., Akemann, W., and Knöpfel, T. (2007). Engineering and characterization of an enhanced fluorescent protein voltage sensor. PLoS ONE *2*, e440.

Elsliger, M.A., Wachter, R.M., Hanson, G.T., Kallio, K., and Remington, S.J. (1999). Structural and spectral response of green fluorescent protein variants to changes in pH. Biochemistry *38*, 5296–5301.

Ilagan, R.P., Rhoades, E., Gruber, D.F., Kao, H.-T., Pieribone, V.A., and Regan, L. (2010). A new bright green-emitting fluorescent protein—engineered monomeric and dimeric forms. FEBS J. *277*, 1967–1978.

Jin, L., Baker, B., Mealer, R., Cohen, L., Pieribone, V., Pralle, A., and Hughes, T. (2011). Random insertion of split-cans of the fluorescent protein venus into Shaker channels yields voltage sensitive probes with improved membrane localization in mammalian cells. J. Neurosci. Methods *199*, 1–9.

Kralj, J.M., Hochbaum, D.R., Douglass, A.D., and Cohen, A.E. (2011). Electrical spiking in Escherichia coli probed with a fluorescent voltage-indicating protein. Science *333*, 345–348.

Kralj, J.M., Douglass, A.D., Hochbaum, D.R., Maclaurin, D., and Cohen, A.E. (2012). Optical recording of action potentials in mammalian neurons using a microbial rhodopsin. Nat. Methods *9*, 90–95.

Lundby, A., Mutoh, H., Dimitrov, D., Akemann, W., and Knöpfel, T. (2008). Engineering of a genetically encodable fluorescent voltage sensor exploiting fast Ci-VSP voltage-sensing movements. PLoS ONE *3*, e2514.

Miesenböck, G., De Angelis, D.A., and Rothman, J.E. (1998). Visualizing secretion and synaptic transmission with pH-sensitive green fluorescent proteins. Nature *394*, 192–195.

Murata, Y., Iwasaki, H., Sasaki, M., Inaba, K., and Okamura, Y. (2005). Phosphoinositide phosphatase activity coupled to an intrinsic voltage sensor. Nature *435*, 1239–1243.

Perron, A., Mutoh, H., Launey, T., and Knöpfel, T. (2009). Red-shifted voltage-sensitive fluorescent proteins. Chem. Biol. *16*, 1268–1277.

Popovic, M.A., Foust, A.J., McCormick, D.A., and Zecevic, D. (2011). The spatio-temporal characteristics of action potential initiation in layer 5 pyramidal neurons: a voltage imaging study. J. Physiol. *589*, 4167–4187.

Sakai, A., Nakayama, M., Numata, M., Takesawa, S., and Nakamoto, M. (2001a). Sodium sulfite and N-acetylcysteine: new additives to dialysate for inhibiting formation of glucose degradation products and advanced glycation end-products. Adv. Perit. Dial. *17*, 66–70.

Sakai, R., Repunte-Canonigo, V., Raj, C.D., and Knöpfel, T. (2001b). Design and characterization of a DNA-encoded, voltage-sensitive fluorescent protein. Eur. J. Neurosci. *13*, 2314–2318.

Sankaranarayanan, S., De Angelis, D., Rothman, J.E., and Ryan, T.A. (2000). The use of pHluorins for optical measurements of presynaptic activity. Biophys. J. *79*, 2199–2208.

Shinobu, A., Palm, G.J., Schierbeek, A.J., and Agmon, N. (2010). Visualizing proton antenna in a high-resolution green fluorescent protein structure. J. Am. Chem. Soc. *132*, 11093–11102.

Siegel, M.S., and Isacoff, E.Y. (1997). A genetically encoded optical probe of membrane voltage. Neuron *19*, 735–741.

Tsutsui, H., Karasawa, S., Okamura, Y., and Miyawaki, A. (2008). Improving membrane voltage measurements using FRET with new fluorescent proteins. Nat. Methods *5*, 683–685.

Villalba-Galea, C.A., Miceli, F., Taglialatela, M., and Bezanilla, F. (2009). Coupling between the voltage-sensing and phosphatase domains of Ci-VSP. J. Gen. Physiol. *134*, 5–14.